ELSEVIER

Contents lists available at ScienceDirect

# Journal of Power Sources

journal homepage: www.elsevier.com/locate/jpowsour





# Towards sustainable interconnects for solid oxide cells: An integrated technical and environmental evaluation of coating methods

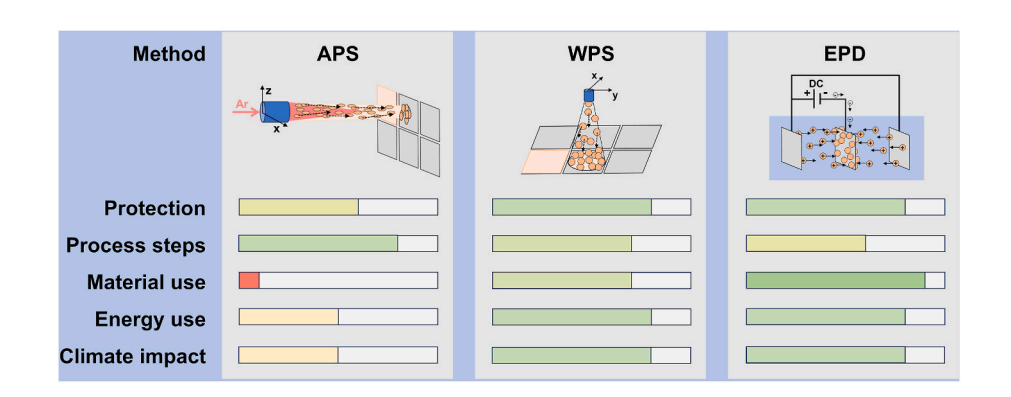
Martin Hilger <sup>a,b</sup>, Khaled El Jardali <sup>c,d</sup>, Vafa Feyzi <sup>c</sup>, Daniil Vakhrameev <sup>e</sup>, Dmitry Naumenko <sup>e</sup>, Ruth Schwaiger <sup>e</sup>, Diego Iribarren <sup>c</sup>, Christian Lenser <sup>a,\*</sup>, Olivier Guillon <sup>a,b,f</sup>, Norbert H. Menzler <sup>a,b</sup>

- a Forschungszentrum Jülich GmbH, Institute of Energy Materials and Devices, IMD-2: Materials Synthesis and Processing, Wilhelm-Johnen-Str., 52425, Jülich, Germany
- <sup>b</sup> RWTH Aachen University, Institute of Mineral Engineering (GHI), Forckenbeckstr. 33, 52074, Aachen, Germany
- <sup>c</sup> Systems Analysis Unit, IMDEA Energy, 28935, Móstoles, Spain
- <sup>d</sup> Rey Juan Carlos University, 28933, Móstoles, Spain
- e Forschungszentrum Jülich GmbH, Institute of Energy Materials and Devices, IMD-1: Structure and Function of Materials, Wilhelm-Johnen-Str., 52425, Jülich, Germany
- f JARA: Jülich-Aachen-Research-Alliance, 52428, Jülich, Germany

#### HIGHLIGHTS

- Alternative coating routes for SOC interconnects evaluated against APS benchmark.
- All coatings provide oxidation protection; WPS and EPD show enhanced performance.
- All methods enable uniform coatings on complex, application-relevant shapes.
- Suspension-based WPS and EPD processes enable reduced material and energy demand.
- Results support WPS and EPD as sustainable and superior protective solutions.

#### GRAPHICAL ABSTRACT



# ARTICLE INFO

Keywords:
Solid oxide cell
Interconnect
Life cycle assessment
Atmospheric plasma spraying
Wet powder spraying
Electrophoretic deposition

# ABSTRACT

This work presents a comprehensive evaluation of three industrially relevant coating processes – atmospheric plasma spraying (APS), wet powder spraying (WPS), and electrophoretic deposition (EPD) – for the application of  $MnCo_{1.9}Fe_{0.1}O_4$  (MCF) spinel-based protective layers on solid oxide cell (SOC) interconnects. Using Crofer-type ferritic stainless steels as substrate, the coatings were assessed with respect to their technical performance and environmental impact. Microstructural characterization, topography analysis for relevant interconnect structures, and mid-term exposure tests at 800  $^{\circ}$ C in air confirm that all three methods can produce uniform, well-adhering, and protective coatings compatible with SOC stack integration. While APS serves as a technologically mature reference, the suspension-based techniques WPS and EPD demonstrate comparable protective functionality after suitable thermal treatments. Furthermore, life cycle assessment reveals significant sustainability benefits for the newer methods – especially EPD – due to lower energy demand and enhanced material

E-mail address: c.lenser@fz-juelich.de (C. Lenser).

<sup>\*</sup> Corresponding author.

efficiency. The results highlight WPS and EPD as promising, environmentally advantageous alternatives for large-scale application of protective interconnect coatings in SOC systems.

#### 1. Introduction

In the global transition towards a net-zero energy system, the vast expansion of renewable energies necessitates substantial advances in energy conversion and storage technologies. Among these, green hydrogen plays a pivotal role. In hydrogen production, a variety of technologies coexist, differing in their applications and scalability. Solid Oxide Cells (SOCs) are of particular interest due to their high efficiencies, notably in combined heat and power systems, and their capability to operate both as fuel cells and electrolyzers (reversible SOCs) [1].

In practical applications, planar SOCs are typically assembled into stacks comprising several cells connected in series. These stacks consist of repeating units that integrate metallic components (mainly interconnects), ceramic cells, contact layers, and gas distribution meshes. The metallic parts are critical, ensuring electrical connectivity between cells while facilitating gas distribution and managing thermal gradients. Ferritic stainless steels with chromium contents of 22–24 mass% are preferred for these components due to their excellent electrical conductivity, self-protecting corrosion behavior through the formation of a chromia scale, and a coefficient of thermal expansion (CTE) well-matched to the ceramic cells.

Even though Cr-rich ferritic stainless steels are specifically tailored for applications in SOC environments, the harsh operating conditions (600–850 °C, partially oxidizing atmospheres and elevated water vapor pressure) impose significant stress on interconnect components during long-term operation. Beyond general oxidation phenomena, so-called "break-away corrosion" – characterized by a sudden increase in electrical resistance and potential contact loss – as well as chromium evaporation at the air-electrode side are considered the dominant degradation mechanisms related to the steel components. Depending on the air-electrode composition, chromium incorporation can lead to secondary phase formation, accompanied by mechanical stress and performance deterioration. In the widely used (La,Sr)(Co,(Fe))O<sub>3</sub> (LSC (F)) air-electrode and contact-layer system, the formation of SrCrO<sub>4</sub> represents the critical degradation pathway [2–4].

To mitigate these effects, dense ceramic protective coatings are widely employed. These coatings not only inhibit the growth of chromia scales but also suppress the evaporation of volatile chromium species into the cell environment [5]. The demands associated with these coatings define a set of specific requirements for both the coating material and the deposition process, including.

- Chemical and thermo-mechanical compatibility with the interconnect steel.
- Low area-specific resistance to minimize ohmic losses in the stack.
- Slowed oxidation kinetics through reduced oxygen ingress.
- Suppression of chromium evaporation.
- Continuous, dense, and homogeneous coatings over complex flow-field geometries. [6,7]

With respect to coating thickness, studies suggest that no strict threshold exists for effective migration barrier functionality; rather, coating density predominantly governs the blocking behavior [8–10]. Consequently, material and process selection should prioritize achieving high coating density, while the minimum thickness primarily depends on ensuring complete substrate coverage.

A wide range of material and coating solutions has been discussed in the literature. Among the potential materials, Mn-based spinels – especially Mn-Co spinels – have emerged as highly suitable candidates owing to their adequate electrical conductivities, thermo-mechanical

compatibility with steel, and exceptional protective properties [11]. While cobalt-containing spinels remain the state-of-the-art reference material for high-temperature SOC interconnects due to their proven stability and compatibility, efforts toward cobalt substitution – e.g., by Cu-based spinels – are gaining attention to reduce environmental impact. However, these alternatives have so far demonstrated promising performance mainly under intermediate-temperature conditions and require further optimization for high-temperature SOC operation [12–14].

A representative state-of-the-art system for steel and coating, developed at Forschungszentrum Jülich for high-temperature SOC conditions, combines Crofer22APU or Crofer22H stainless steels with a Fe-doped Mn-Co spinel (MnCo<sub>1.9</sub>Fe<sub>0.1</sub>O<sub>4</sub>, MCF) as the ceramic protective layer [15,16]. Regarding deposition methods, a range of techniques has been explored in literature, including screen printing, various physical vapor deposition (PVD) processes, and thermal spraying [6,9,17–21]. Among these, atmospheric plasma spraying (APS) is the established reference process at Forschungszentrum Jülich, offering excellent coating quality and long-term stability exceeding 30,000 h. However, alternative methods – especially those with potential advantages in cost efficiency and ecological impact – are attracting increasing attention [22].

Due to the substantial coating thickness ( $\sim 100~\mu m$ ) and energy-intensive nature of the APS technology, alternative deposition techniques suitable to apply thinner ceramic coatings ( $\sim 1-10~\mu m$ ) and for scalable industrial application are being explored. In this context, wet powder spraying (WPS) and electrophoretic deposition (EPD) are particularly promising, enabling thin, uniform coatings on complex-shaped metal substrates. Both methods are already established in mass production across various sectors, such as furniture, domestic appliances, automotive, and biomedical industries, due to their high coating uniformity, flexibility, and cost efficiency [23–26]. Their suitability for applying Mn-based spinel coatings on SOC interconnects and their promising performance have been demonstrated in multiple studies, highlighting them as viable alternatives to APS [15,27–29].

While significant research has focused on the solid oxide cells and overall stack performance, the environmental implications and efficiency of coating processes for interconnects remain insufficiently addressed, despite their critical influence on system durability and resource demand. In particular, systematic studies that combine detailed technical evaluation with a life cycle assessment of relevant and scalable coating processes are largely absent from the literature, representing a substantial knowledge gap.

This work systematically compares the methods APS, WPS, and EPD in terms of coating quality, functionality, and environmental sustainability. State-of-the-art materials, namely MCF for the protective layer and Crofer22APU/H for the steel substrates, are employed. Coating microstructures – including density, continuity, homogeneity, and integrity – are characterized on flat and structured substrates to validate their functionality. The microstructural characteristics are investigated along the thermal treatments specific to each coating type – the intrinsic oxidation during stack operation for APS, and an additional extrinsic reduction step (2 h at  $1000~{\rm C}$  in Ar/2.9 % H<sub>2</sub>) for WPS and EPD.

Furthermore, chromia scale growth after 3000 h of exposure under SOC air-side conditions is investigated to assess the protective performance of each coating type. Subsequently, a detailed environmental sustainability assessment is conducted using life cycle assessment (LCA), encompassing the entire processing chain up to the coated interconnect component. Waste and energy flows are mapped and quantified throughout the production steps. Environmental impacts – including acidification, use of minerals and metals, use of fossil resources, and

climate change – are calculated. By comparing and scaling the results to the production of a single interconnect sheet, this study provides a comprehensive basis for a sustainability-driven selection of the most appropriate coating technique, suitable for a representative interconnect shape and size.

#### 2. Methodology

#### 2.1. Materials

#### 2.1.1. Stainless steel

For the stainless-steel substrates, ferritic stainless steels Crofer22APU and Crofer22H have been selected. These steels constitute state-of-the-art materials for use as SOC interconnects and were specifically developed for this purpose [6,30]. Their pronounced suitability is attributed to a well-matched CTE (cf. Section 2.1.2) with the ceramic cell components, high electrical conductivity, and excellent corrosion stability under SOC operating conditions. The latter results from their comparatively high chromium content of around 22 mass%, promoting the formation of a stable, self-passivating chromia scale ( $\text{Cr}_2\text{O}_3/(\text{Mn}, \text{Cr})_3\text{O}_4$ ). Crofer22H, the most recently developed variant, features enhanced mechanical properties, particularly improved creep resistance, due to the precipitation of intermetallic Laves phases rich in W, Nb, and Si [31,32]. Consequently, Crofer22H is of particular interest for thin-sheet applications, which are increasingly required by modern lightweight interconnect designs.

Within this study, Crofer22APU was used as the base material for coating demonstrations on real flow-field structures, consisting of cutouts from an established Jülich interconnect design with challenging, sharp-edged topographies. Crofer22H served as the substrate for microstructural characterization and corrosion testing, as it is the candidate of pronounced relevance for modern, light-weight interconnect designs. The compositions of both steel types, along with their CTE values at 800  $^{\circ}$ C, are listed in Table 1.

#### 2.1.2. Spinel powders

The spinel composition selected as coating material in this study is MnCo<sub>1.9</sub>Fe<sub>0.1</sub>O<sub>4</sub> (MCF), a candidate from the (Mn,Co)<sub>3</sub>O<sub>4</sub> spinel family, which represents a promising material group for interconnect protective coatings [11]. The relevant properties of the material lie in its CTE of  $13.4 \times 10^{-6} \, \text{K}^{-1}$ , which matches well with that of ferritic stainless steels and ceramic cell components, typically ranging between 10 and 13 imes10<sup>-6</sup> K<sup>-1</sup>, and its comparatively high electrical conductivity (72 S cm<sup>-1</sup>) [35,36]. Moreover, when applied via APS, long-term stability and even self-healing properties during operation under SOC air-side conditions have been reported [22,37]. The use of MCF as reference material in this study is motivated by its well-established performance for high-temperature SOC operation, ensuring a robust basis for comparing alternative coating processes. While the environmental impact of cobalt is acknowledged, selecting this material enables benchmarking against the current state-of-the-art. Recent research has explored Cu-Mn spinels as cobalt-substituting candidates to mitigate environmental concerns; however, these compositions have shown sufficient stability mainly for intermediate-temperature SOCs, and their applicability under the high-temperature conditions addressed here remains limited [12-14].

Additionally, long-term experience with MCF-based APS coatings provides a broad reference for evaluating alternative deposition techniques in terms of technical performance and durability. According to the specific requirements of the three coating methods, different powder properties relating to particle size and morphology are necessary. While the APS process demands relatively large particles with diameters in the range of approximately 10–100 μm to ensure proper material transport and deposition, finer particles (~1 µm and below) are essential for WPS and EPD to achieve homogeneous deposition. For WPS, the suspension, composed of spinel powder and several organic components, must be dispersible and suitable for continuous atomization and spraying through a nozzle. In contrast, for EPD, even smaller particles in the submicron range are generally required, as the driving force for material transport by electrophoretic motion is closely related to the induced surface charges. Beyond the powder properties, these surface charges are significantly influenced by the suspension components themselves, with an essential distinction between aqueous and non-aqueous systems. Non-aqueous, organic suspensions, utilizing stabilizing agents, allow the use of larger particles, while aqueous suspensions typically require particle sizes around or below 500 nm. This is due to their lower ionic strength and the stronger tendency for agglomeration and sedimentation in aqueous media, whereas smaller particles provide higher electrophoretic mobility owing to an increased surface area per unit mass. For EPD in general, precise adjustment of the particle size distribution according to the suspension system is critical for achieving uniform and homogeneous coatings [38,39].

For the preparation of APS coatings, commercial MCF powder manufactured by H.C. Starck (Selb, Germany) was used. The WPS and EPD coatings are based on commercial powder produced by KCeracell (Pyeongtaek, South Korea). For the EPD process, an additional milling step was performed to achieve the required particle size distribution. This treatment was conducted using a planetary ball mill of the type Pulverisette 7 (manufacturer: Fritsch GmbH, Idar-Oberstein, Germany). Milling was carried out in ethanol with 1 mm diameter yttria-stabilized zirconia (YSZ) balls. For each run, 10 g of MCF powder was treated with 100 g YSZ balls in 25 ml ethanol. Milling was performed at 500 rpm for 60 min. After treatment, the powder was dried and manually deagglomerated using a mortar.

An overview of the powder characteristics, including particle size distributions and representative scanning electron microscopy (SEM) images, is shown in Fig. 1. The characterization procedure of the powders is detailed in Section 2.3.1.

# 2.2. Coating methods

This chapter provides an overview of the methodologies and specifications of the three coating techniques (APS, WPS, and EPD), with special focus on the application of MCF coatings. The key processing steps relevant for both the coating characteristics and the LCA study are explained and contrasted. A schematic representation introducing the three coating methods, highlighting the most relevant process steps as well as energy, mass, and waste flows, is presented in Fig. 2. Data acquisition for the LCA study was conducted along the respective process chains, while a detailed description of the procedure, including a schematic focusing on the hotspots of material and energy consumption,

Table 1 Chemical composition and CTE (at 800 °C) for Crofer22APU and Crofer22H [33]. [34].

		Fe	Cr	C	N	S	Mn	Si	Ti	W	Nb	Cu	P	Ni	Al	La	CTE
		_	(%)	(%)	(%)	(%)	(%)	(%)	(%)	(%)	(%)	(%)	(%)	(%)	(%)	(%)	$10^{-6}~{ m K}^{-1}$
Crofer22APU	min	Bal.	20.0	0.03	-		0.30		0.03	-	-			-		0.04	11.9
	max		24.0		-	0.02	0.80	0.50	0.20	-	-	0.50	0.05	-	0.50	0.20	
Crofer22H	min	Bal.	20.0	0.03				0.10	0.02	1.0	0.20					0.04	11.8
	max		24.0		0.04	0.006	0.80	0.60	0.20	3.0	1.0	0.50	0.50	0.50	0.1	0.20	

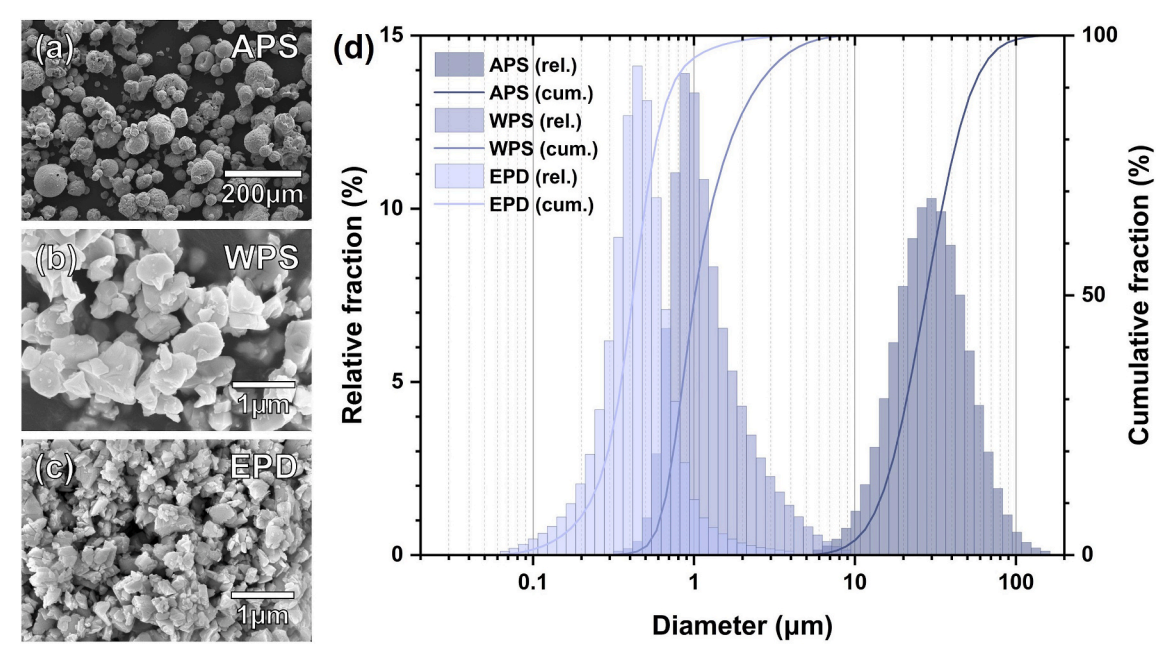


Fig. 1. Characteristics of the MCF spinel powders used for the coating processes demonstrating the differences in particle size and distributions for the three deposition methods: Secondary electron SEM images of the powders for (a) APS, (b) WPS, and (c) EPD; and (d) particle size distribution analysis via laser diffraction.

is given in Section 2.4. For completeness, key process characteristics for APS and WPS are summarized below to complement the schematic representation, whereas the EPD methodology is explained in greater detail due to its novel implementation in this study.

#### 2.2.1. Atmospheric plasma spraying (APS)

APS is a thermal spray coating technique in which powdered materials are injected into a high-temperature plasma jet, where they are heated and propelled onto a substrate. When applied to ceramic powders, coating thicknesses typically range from a few tens of micrometers up to 1 mm [40]. APS coatings are characterized by good adhesion and thermo-mechanical stability. However, the comparatively large coating thicknesses and overspray limit material efficiency, while the operation of a plasma torch results in considerable energy consumption. Relevant process parameters for spraying ceramic APS coatings onto steel substrates include plasma power, feedstock powder characteristics, gas flow rate, spray distance, and substrate temperature. These parameters significantly influence coating adhesion, density, microstructure, and overall performance [40,41].

The MCF-APS coating type, established and successively developed at Forschungszentrum Jülich since 2007, represents herein a state-ofthe-art reference for interconnect coatings in SOC research [19,42]. These coatings have been incorporated into numerous stack runs, proving their excellent functionality and suitability for long-term operation [22,43,44]. The APS methodology used in this study is fully based on this optimized process. The coatings were applied using a Triplex Pro 210 gun within a multi coat facility (manufacturer: Oerlikon Metco, Wohlen, Switzerland) operating with Ar/He as the primary plasma gases and employing a standard powder feeding system. The MCF feedstock consisted of a monomodal spinel powder (d50  $\approx$  27  $\mu$ m), ensuring stable flowability during spraying. Further technical details and information on the working principle of the coatings can be found elsewhere [37,45]. It is worth noting that the MCF-APS coatings for all Jülich stack components are now applied by an external industrial partner, demonstrating the process's industrial scalability.

During deposition, reducing conditions in the plasma torch cause partial reduction of the  $(Mn,Co,Fe)_3O_4$  spinel phase to the  $(Mn,Co,Fe)_1O_1$  rock salt phase. This enables further densification through in-situ re-oxidation during operation in SOC air-side atmospheres [37].

Consequently, no additional thermal post-treatment of the coating is necessary, as densification is achieved during the stack assembly and sealing process, performed over 100 h at 850  $^{\circ}\mathrm{C}$  in air. During this step, the stack components are joined using a glass sealant to create a gas-tight and insulating, finally glass-ceramic, connection prior to operation.

#### 2.2.2. Wet powder spraying (WPS)

WPS is a process where a suspension of fine ceramic or metal powders, typically mixed with a binder and solvent, is atomized and sprayed onto substrates to form continuous ceramic coatings. The ceramic powder provides the desired material properties, while the binder stabilizes the suspension and promotes particle adhesion during spraying. The solvent adjusts the viscosity of the suspension to enable efficient spray application and uniform coating formation. The choice of binder and solvent is critical for achieving optimal coating quality and uniformity. After drying and thermal treatment, the volatile (organic) components are removed, while the densified, pure ceramic coating remains on the substrate. Typically, ceramic coatings produced by WPS range from a few up to several tens of micrometers or even 100  $\mu m$ . The technique is particularly suitable for depositing thin, continuous ceramic coatings on large-scale and structured components. While heat treatments are necessary for the deployment of WPS-coated components, appropriate thermal processing steps can also be chosen to tailor the microstructural properties as desired [46,47].

In the field of interconnect protective coatings, the WPS technique was introduced early and yielded remarkable results using the basic  $\rm Mn_3O_4$  spinel composition, providing sufficient protection as a Cr-getter layer in a 100 kh solid oxide fuel cell stack run at Forschungszentrum Jülich [15,48]. Based on the more recently established MCF composition adapted from APS coatings, Wolff et al. developed an MCF-WPS coating and reported favorable microstructures and protective properties in 2024 [27]. The coating process applied in this study follows the methodology proposed in this work, using an ethanol-based suspension system containing organic binder and appropriate plasticizers, namely ethoxylated alcohol, polyvinyl acetate and triethylene glycol, to ensure particle stabilization. The suspension was homogenized via ball milling prior to spraying to achieve a uniform distribution of the MCF powder.

Unlike APS coatings, WPS coatings are initially deposited in a loose,

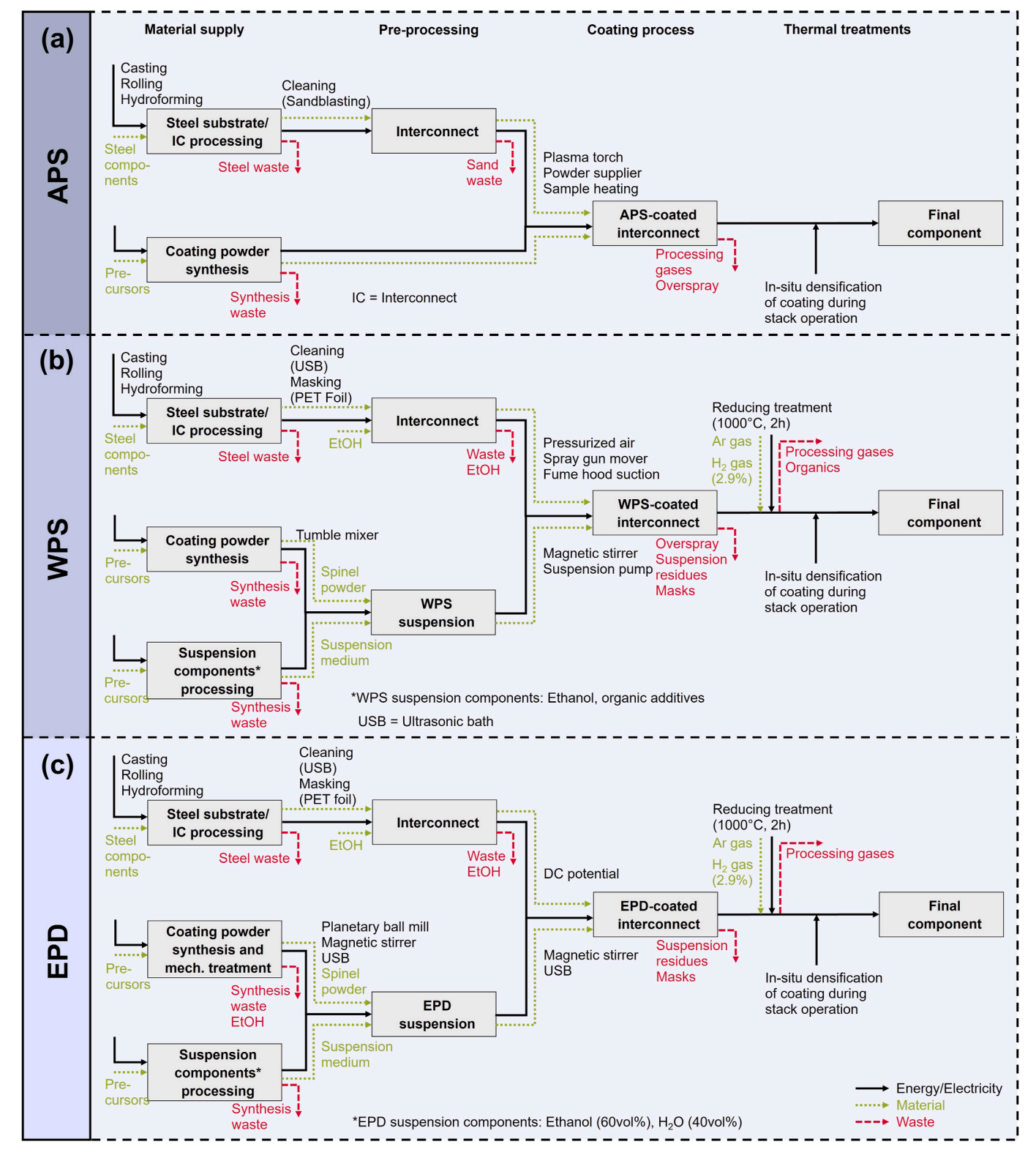


Fig. 2. Flowcharts of the coating processes investigated: (a) APS, (b) WPS, and (c) EPD, with process-relevant positions disaggregated by energy, material, and waste flows.

non-densified (so-called "green") state and require subsequent heat treatment to achieve stability and desired properties. Thermal treatments can be used to remove the residual organic components in the coating and sinter the deposited powder to a continuous, dense layer. It has been shown in various works that two-step treatments, including a first step in reducing atmospheres (containing H<sub>2</sub>) and a subsequent one

in oxidizing atmospheres (as air), are beneficial to achieve this goal [9, 49]. Based on previous optimization efforts, a reductive treatment in Ar/2.9 %  $H_2$  was performed for 2 h at 1000 °C with heating and cooling rates of 5 K min $^{-1}$ , followed by re-oxidation at 850 °C for 100 h under identical ramp rates.

This oxidation step was intentionally designed to simulate the

conditions during SOC stack-assembly, during which the components are joined together with a glass sealant. By integrating the densification of the WPS coatings into the stack-assembly process, an additional high-temperature oxidation treatment of the entire stack components can be omitted. This is critical because certain uncoated regions of the interconnects – essential for electrical contacting to the fuel electrode and for sealing purposes at the stack edges – must remain free of corrosion. Therefore, the combined approach of coating densification and stack-assembly ensures the protective functionality of the coatings while preventing unwanted oxidation of uncoated, functional areas.

# 2.2.3. Electrophoretic deposition (EPD)

EPD is a suspension-based coating method in which charged particles are transported through a polar medium under an applied voltage, enabling the deposition of ceramic layers onto conductive substrates. Since the process occurs in a liquid phase, it is not limited by a line-ofsight effect, allowing for the formation of highly uniform and conformal coatings even on substrates with complex geometries. The thickness and microstructure of the deposited layers can be precisely controlled by adjusting parameters such as suspension composition, solid content, particle morphology and size, applied potential, and deposition time. This enables the fabrication of both porous and dense coatings with thicknesses ranging from a few to several tens of micrometers or even around 100 µm [38]. As in WPS, appropriate heat treatments are crucial for achieving mechanically stable and continuous coatings. This is especially critical for EPD, as the deposition typically occurs without the use of form-stabilizing organic additives, leaving the particle network initially in a loosely packed state prior to sintering.

The suitability of EPD for the fabrication of interconnect protective coatings has been demonstrated in numerous studies, including its transfer to real components and even its application in full stack assemblies [28,29]. A comprehensive review of related research has been provided by Zanchi et al. [50] While alternative coating materials to the established compounds are being explored, the majority of studies still focus on the well-proven (Mn,Co)<sub>3</sub>O<sub>4</sub> spinel and its tailored modifications [50–53].

Various organic solvents, such as ethanol, acetone, and isopropanol, as well as their mixtures, are commonly used as suspension media [50]. To facilitate material transport and suspension stabilization, the addition of surface charge enhancers, typically iodine (I<sub>2</sub>), is required [54]. Additionally, suspension systems incorporating water alongside organic solvents have been established, as the inherent polarity of water induces surface charge formation, eliminating the need for charge-enhancing additives. Numerous studies employing aqueous systems are methodologically based on the process first described by Smeacetto et al. (2015) [55], which utilizes a water-ethanol medium [56–59].

The above-mentioned procedure [55] serves as the foundation for the EPD coatings developed in the present study and has been further optimized for the specific MCF powder used. A suspension medium comprising 60 vol% ethanol and 40 vol% deionized water was employed. The powder was dispersed at a solid content of 40 g  $\rm L^{-1}$  and the resulting suspension was stabilized for the EPD process using magnetic stirring and ultrasonic treatment. After adding the powder to the medium, the suspension was stirred for 30 min, followed by an additional 30 min of ultrasonic treatment (Sonorex Digitec, manufacturer: Bandelin, Berlin, Germany), during which manual stirring was performed for 1 min every 5 min. To enable multiple uses of the suspension for coating several samples, reconditioning was performed by subjecting the suspension to 10 min of ultrasonic treatment along with 1 min of manual stirring immediately before the deposition process. During the deposition, the suspension remained static.

In the EPD setup, the substrates to be coated were positioned parallel to the counter electrodes in a three-electrode configuration and electrically connected using alligator clips. The counter electrodes, made of Crofer22H, were placed at a distance of 1.5 cm on either side of the substrate. The voltage was supplied by a three-channel laboratory power

supply of type 2230-30-1 (manufacturer: Keithley Instruments, Solon, Ohio, USA) and set to 40 V. The deposition time was 45 s for flat substrates and 60 s for structured sheets, accounting for their increased surface area compared to the flat counter electrodes. Prior to heat treatment, the coatings were air-dried for at least 1 h. Analogous to the WPS method, the coated substrates underwent an optimized two-step heat treatment protocol to achieve coating densification.

It should be noted that the coatings investigated in this study differ in thickness, reflecting the inherent characteristics and optimization status of each deposition route. In particular, APS coatings are intentionally applied with comparatively high thickness, as they represent the long-standing reference configuration established through extensive stack testing and proven for reliable performance in service. Consequently, this work focuses on comparing these coating technologies in their optimized, practically relevant forms, rather than artificially adjusting the layer thickness for uniformity.

# 2.3. Characterization methods

# 2.3.1. Starting powders

To determine the required particle sizes and morphologies for the three coating processes, SEM and laser diffraction were employed. SEM imaging was performed using a GeminiSEM (manufacturer: Zeiss, Oberkochen, Germany) system equipped with a field emission electron source. Secondary electron (SE) detection was applied to obtain topographic contrast. Powders were dispersed on conductive carbon tape to ensure sufficient electrical conductivity and adhesion within the vacuum chamber during imaging.

Particle size distributions (PSD) were determined using a laser diffraction particle size analyzer (LA-950V2, manufacturer: Horiba, Kyoto, Japan) operating with 405 nm and 650 nm laser wavelengths. Depending on particle size, different evaluation models were applied: coarse APS powders were analyzed using Fraunhofer theory, while finer WPS and EPD powders were evaluated using Mie theory, assuming a refractive index of 2 for the MCF material.

#### 2.3.2. Flow-field structures

In typical interconnect designs used in SOC stacks, the gas distributor or flow-field structures represent critical zones for protective coatings. On the one hand, these regions are in direct contact with the cell on the air side and are simultaneously exposed to a continuous and aggressive flow of oxygen-containing atmospheres at operating temperatures exceeding 800 °C, imposing stringent requirements on the protective effectiveness of the coating. On the other hand, the complex geometries of the flow-field structures, which can feature sharp-edged profiles, present significant challenges for the deposition of uniform and defect-free coatings, especially for line-of-sight processes such as APS or WPS.

Therefore, to evaluate the suitability of the three coating techniques, MCF-based coatings were applied onto representative flow-field structures and analyzed regarding their integrity and continuity. For this purpose, a classical flow-field design of the Jülich F10-type interconnect was selected. This structure not only represents a standard in stack-level testing but also provides particularly demanding conditions for achieving high coating qualities due to its sharp-edged rib-channel structure, which is milled directly from bulk material. Fig. 3 provides a schematic overview of the investigated interconnect geometry and its integration, together with the coating, into the SOC stack.

In this study, segments of the respective flow-field structures with dimensions of 25 mm  $\times$  25 mm (cf. Fig. 3c) were coated using the alternative methods WPS and EPD and subsequently compared to a reference sample coated by APS (in the form of an F10-type interconnect coated according to the standard procedure). The comparison was carried out on samples in the state prior to stack integration. Topographic analyses were performed using a laser scanning confocal microscope (type VK-X160K, manufacturer: Keyence Corp., Osaka, Japan) over a representative area of a repeating unit of the rib-channel structure,

Fig. 3. Schematic of single repeating unit in a fuel electrode supported SOC stack: (a) exploded diagram and (b) cross-section. (c) Cutting of Jülich-type flow-field structure (Crofer22APU).

whereby nine individual images per sample were stitched together to obtain a comprehensive view.

#### 2.3.3. Evolution of microstructures

Although the three coatings compared within this study are based on the same material composition, significant differences in the resulting coating microstructures can arise. These differences are primarily attributed to the pronounced variations in the employed feedstock powders, particularly regarding particle sizes and morphologies, as well as to the specific characteristics of the respective coating processes, including their thermal treatments. In particular, the reducing conditions and the high particle velocities inherent to the APS process, as well as the pre-reduction of the WPS and EPD coatings prior to subsequent processing, represent critical factors influencing the final coating properties.

To evaluate the resulting coating qualities in terms of continuity, integrity, and density, microstructural analysis was performed on metallographic cross sections. The characteristic microstructures of the three coating types were systematically compared at relevant processing stages. For this purpose, WPS and EPD coatings were applied to Crofer22H substrates (dimensions:  $25~\text{mm} \times 25~\text{mm}$ , thickness: 0.3~mm) and analyzed both in the reduced state and after the subsequent assembly step. APS-coated specimens were cut from a  $50~\text{mm} \times 50~\text{mm}$  plate (thickness: 2~mm) by laser cutting and served as source material for all characterization and testing purposes within this study. For the specific microstructural analysis described here, segments with dimensions of  $10~\text{mm} \times 10~\text{mm}$  were prepared from these APS-coated plates.

For the preparation of cross-sections, samples were embedded in epoxy resin, followed by automated, multi-step grinding and polishing. Prior to embedding, the oxidized samples were electroplated with Ni to minimize damage to the coating during sample preparation and to enhance contrast in the microstructural characterization. Imaging was performed analogously to the powder characterization using a microscope of the type GeminiSEM, utilizing secondary electrons to visualize structural features. Within the microstructural cross section characterization, complementary analysis of the elemental distribution in the relevant processing steps is performed via energy dispersive X-ray spectroscopy (EDS).

#### 2.3.4. Proof of protectivity

To evaluate the fundamental protective functionality of the three coating types, long-term exposure tests of coated and uncoated Crofer22H substrates under oxidizing conditions were conducted, followed by subsequent microstructural analysis. For this purpose, specimens with dimensions of 20 mm  $\times$  10 mm, including a 2.5 mm hole near the edge, were cut from the coated and heat-treated substrates (25 mm  $\times$  25 mm for WPS and EPD, and 50 mm  $\times$  50 mm for APS) using laser cutting. While the thin 0.3 mm WPS- and EPD-coated sheets were symmetrically coated on both sides to prevent asymmetric corrosion effects and deformation during exposure, this was not required for the APS-coated substrates. Due to the increased substrate thickness of 2 mm, potential asymmetry effects from backside oxidation can be avoided, allowing for coating on only one side.

The exposure tests were carried out at 800  $^{\circ}\text{C}$  in ambient air for a total duration of 3000 h. During exposure, the samples were suspended

on  $Al_2O_3$  tubes inside a horizontal high-temperature tube furnace (manufacturer: Carbolite Gero, Hope Valley, England). To assess the protective effect of the coatings in comparison to uncoated steel, a qualitative evaluation was performed based on SEM and EDS analyses on cross sections, conducted on the SEM system Merlin (manufacturer: Zeiss, Oberkochen, Germany) following the procedure described in Section 2.3.3.

The EDS analysis enables the assessment of both the coatings' barrier effectiveness against chromium diffusion and the corrosion protection of the steel substrate. Moreover, it provides insights into the phase stability of the three coatings over the course of mid-term exposure.

#### 2.4. Environmental life cycle assessment framework

LCA is a holistic methodology to evaluate the potential environmental impacts of a product system. It allows a comprehensive identification of the hotspots that should be addressed to enhance the system's environmental performance. The standardized LCA methodology comprises four interrelated stages: definition of the goal and scope of the assessment, life cycle inventory (LCI) analysis, life cycle impact assessment, and interpretation of results [60].

The goal of this LCA study is to characterize and compare the environmental performance of three different coating techniques for interconnects used in SOCs: APS, WPS, and EPD, as presented in Section 2.2. Moreover, this study aims to identify the corresponding environmental hotspots where improvements should be focused for future large-scale application and technology commercialization. In order to facilitate the comparison of the environmental profiles, the functional unit was defined as 175 cm<sup>2</sup> of coated area, which corresponds to a typical pilot-scale SOC stack interconnect size. The coating plant was assumed to be located in Germany.

The coating systems under study (Fig. 4) encompass raw material acquisition, coating powder production and the preparation of coating suspensions, including mask preparation and the final steps for heat treatment of the coated substrates. It should be noted that, given the research focus on the coating technique itself, the substrate to be coated was not considered within the system boundary.

Data on mass and energy flows for the processes within the foreground system in Fig. 4 were based on the experimental work explained in Section 2.2, supplemented by literature data and adapted to industrial application as explained below. The corresponding inventory data are presented in Table 2. It should be noted that the values per functional unit in Table 2, except for electricity consumption, could remain valid under equivalent assumptions regardless of production scale. The synthesis of MnCo<sub>1.9</sub>Fe<sub>0.1</sub>O<sub>4</sub> (MCF) powder for the three coating methods was based on the work of El Jardali et al. [61] For APS, the powder is heated and fed into a plasma torch and then coated on a substrate. Unlike APS, WPS and EPD follow a similar coating approach that involves suspension synthesis, mask preparation, coating processes coupled with magnetic stirring and treatment in an ultrasonic bath (USB), and finally furnace reduction. Materials and energy consumption data for USB cleaning and EPD coating were adjusted by considering periodic replacement of the USB fluid and EPD suspension solvents. It was assumed that ethanol used for USB cleaning is changed after 6 h of continuous use, while the suspension solvent (ethanol + deionized

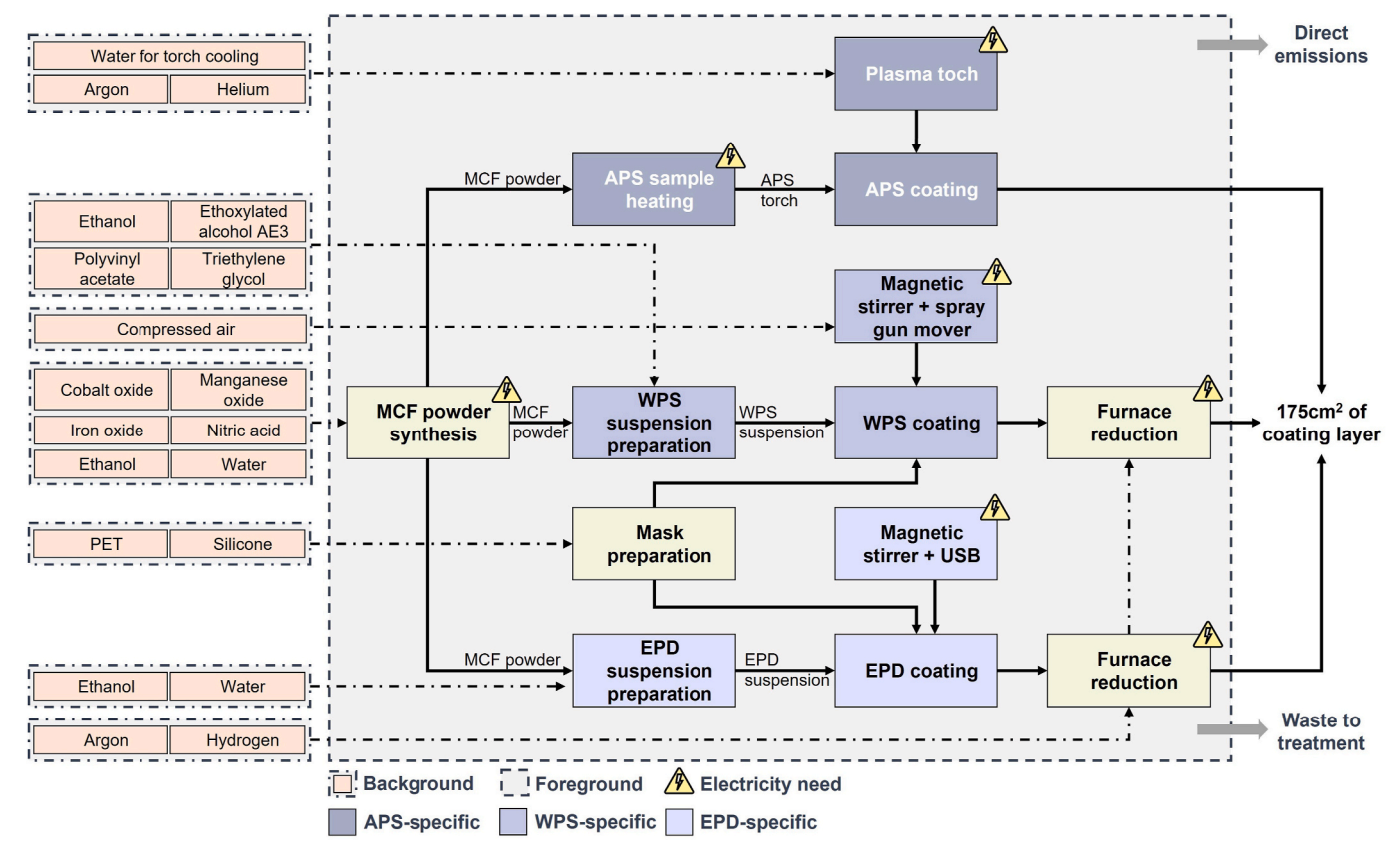


Fig. 4. Schematic of the foreground and background processes and streams within the three coating systems under investigation.

water) is renewed after every ten coating cycles in the EPD process. Electricity consumption in each system was calculated according to the power of the involved machines and their utilization time for each processing step. Continuous electrical furnaces were considered for the reduction of the coated substrates in WPS and EPD processes. The electricity consumption in the reduction furnaces was estimated based on the adjusted conveyor speed, heating and cooling rate, reduction temperature and time, and the furnace dimension [62]. Finally, inventory data for background processes such as waste management and chemicals production were retrieved from the ecoinvent database [63].

The established inventories were implemented in the software SimaPro® for the subsequent environmental characterization of each coating system. Environmental Footprint 3.1 was used as the environmental characterization method following the recommendations of the European Commission [64]. In particular, four environmental indicators were evaluated: the carbon footprint of each coating technique (i.e., climate change, in kg  $CO_2$  eq), acidification (mol  $H^+$  eq), use of fossil resources (MJ), and use of minerals and metals (kg Sb eq).

#### 3. Results and discussion

#### 3.1. Characterization of initial state

The qualitative comparison of surface topographies using confocal laser scanning microscopy aims to evaluate the coatings' continuity and integrity and thus demonstrate the suitability of the three deposition methods for applying protective coatings on relevant flow-field structures. The respective coating types, applied to Crofer22APU cut-outs with rib-channel structures, were analyzed in the condition in which they are intended to be integrated into a SOC stack. The resulting stitched images are presented in Fig. 5.

The topography analysis revealed continuous coatings deposited across all characteristic regions within the repeating unit of the rib-

channel structure. Nevertheless, distinct differences between the APS method and the suspension-based processes, WPS and EPD, are evident in terms of surface roughness and shape fidelity, particularly in the edge regions. Despite these differences, coherent and fully covering coatings were achieved in all cases. Variations in the starting powders, deposition mechanisms, and the influence of subsequent thermal treatments may lead to differences in coating thickness, especially in characteristic structural regions such as convex edges or flanks.

However, previous investigations on interconnect coatings have emphasized that the decisive criterion for ensuring reliable oxidation protection is the presence of a continuous, adherent layer rather than uniform thickness, also counting for sharp-corner regions [8–10]. The topography investigations confirm that the principal requirement of consistent deposition of a continuous coating is met for all three coating processes. Furthermore, the feasibility of achieving such coverage on real interconnect geometries, including flow field structures, has been demonstrated in earlier studies for all three methods [22,27,28]. Accordingly, the investigations reaffirm that all three methods are, in principle, suitable candidates for the application of protective coatings on complex-shaped gas distribution structures in SOC interconnect flow fields – even when challenging topographies with sharp edges and steep slopes are involved, as now comparatively demonstrated on the identical rib-channel structure.

The investigation of the coatings' microstructural evolution by means of metallographic cross sections of coated steel substrates provides insights into coating densification and structural characteristics in the final component, i.e., the coated interconnect. Cross-sectional SEM images of MCF-coated Crofer22H substrates at the relevant processing stages – after deposition (APS) or reductive treatment (WPS, EPD), as well as after the assembly protocol – are contrasted in Fig. 6.

Although the micrographs clearly illustrate the pronounced differences in the microstructures evolving throughout deposition and subsequent thermal treatments – further distinguishing between thermal

**Table 2**Main inventory data of the coating systems (values for 175 cm<sup>2</sup> of coated area).

Input from technosphere	Value	Unit	Output	Value	Unit
Atmospheric plasma	spraying (A	APS)			
Helium	1.213	g	Product coated area	175	cm [2]
Argon	109.5	g	Waste paint to treatment	20.7	g
MCF powder	27.50	g	Waste sand to treatment	81.9	g
Electricity	1.360	kWh	Direct argon emission to air	109	g
			Direct helium emission to air	1.2	g
Wet powder spraying	(WPS)				
Ethanol	9.660	g	Product coated area	175	cm [2]
Ethoxylated alcohol (AE3)	0.046	g	Waste paint to treatment	1.45	g
Polyvinyl acetate	0.028	g	Wastewater to treatment	234	g
Triethylene glycol	0.469	g	Direct argon emission to air	156.6	g
Argon	159.6	g	Direct ethanol emission	9.4	g
Compressed air	9.770	1			
Hydrogen, gaseous	0.241	g			
Polyethylene terephthalate (PET)	0.002	g			
Silicone	0.002	g			
MCF powder	0.936	g			
Electricity	1.799	kWh			
Electrophoretic depos					
Ethanol	0.943	g	Product coated area	175	cm [2]
Water, deionized	0.801	kg	Wastewater to treatment	234	g
Argon	159.6	g	Direct argon emission to air	155.9	g
Hydrogen	0.241	g	Direct ethanol emission	0.855	g
MCF powder	0.490	g			
Polyethylene terephthalate (PET)	0.002	g			
Silicone	0.002	g			
Electricity	1.786	kWh			

spray and suspension-based coating techniques –, all three processes demonstrate the capability to generate dense and well-adhering layers after completion of the stack assembly procedure. For each of the processes, the formation of continuous layers with closed porosity can be observed after the re-oxidation treatment.

In the case of the APS process, cracks formed during deposition under reducing conditions are locally healed by a phase transformation of the MCF material from the rock-salt structure into the spinel phase during re-oxidation, thereby leading to a closed porosity (cf. Fig. 6a). In contrast, the partially reduced state of WPS and EPD coatings after the reductive pre-treatment promotes enhanced sinterability and densification during subsequent re-oxidation (cf. Fig. 6b–c). This mechanism, referred to as "reactive sintering", is attributed to the enhanced mobility of the metallic components, Co and Fe, which appear as bright, spherical phases in the SE images. During re-oxidation, these metallic phases reincorporate into the partially reduced MnO matrix and contribute to the re-formation of the MCF spinel structure, thus enhancing densification [9,49].

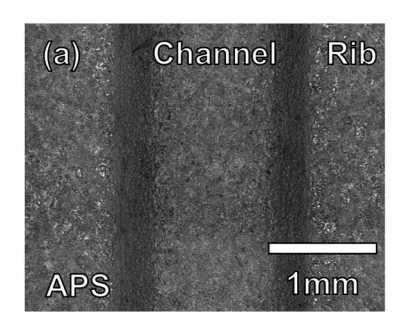
Not only do WPS and EPD coatings show a multi-phase constitution during thermal processing, but the APS coating also exhibits the presence of several phases, though only after the assembly procedure. As stated before, the phase transformation from (Mn,Co,Fe)<sub>1</sub>O<sub>1</sub> to (Mn,Co, Fe)<sub>3</sub>O<sub>4</sub> initially occurs in areas of microcracks, inducing self-healing through volume expansion. As this blocks oxygen pathways through the coating, the further transformation of the bulk material into the spinel phase proceeds via solid-state processes. Due to the large coating thicknesses limiting the kinetics, the full phase transformation of the entire layer exceeds the assembly time of 100 h. During this transition, a temporary top layer dominated by the Co<sub>3</sub>O<sub>4</sub> phase forms, as indicated by EDS analysis (cf. Fig. 6a), which can later fully re-incorporate into the (Mn,Co,Fe)3O4 phase. Though the process is not complete after assembly, the resulting dense microstructure already provides the required protection against the uncontrolled migration of gaseous oxygen and chromium species at the start of operation. A detailed description of the thermodynamic processes and microstructural development of the MCF-APS coating is reported by Grünwald et al. [37].

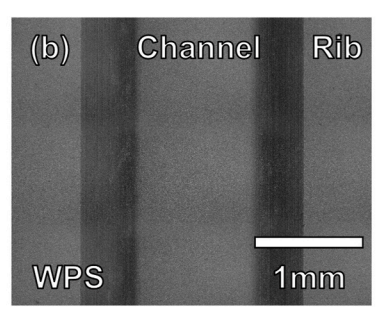
In fact, differences between the coating methods concerning microstructural and phase evolution as well as the overall shape of the coatings – especially between the reference method APS and the suspension-based coating types WPS and EPD – are evident. These differences could be characterized and described in greater detail; however, this is not the focus of the present work. In-depth analysis of similar systems can be found in various works cited above. Importantly, these variations are not crucial to prove the suitability of the coating types for application as interconnect protective coatings. Rather, it is far more critical – besides adaptability to relevant structures – to demonstrate the protective functionality of the coatings under air-side operating conditions.

#### 3.2. Characterization after exposure under operating conditions

After 3000 h of exposure at 800  $^{\circ}$ C in air, the Crofer22H sheets were analyzed by metallographic cross sections using SEM and EDS to evaluate the coating performance. The results for the three coating types are contrasted with bare steel in Fig. 7.

For all three coating types, only minor chromium diffusion into the coating and a limited oxidation rate compared to the bare Crofer22H steel are observed. While differences between the coating types are evident in terms of oxide scale constitution and thickness, the basic protective functionality can be confirmed for all three candidates.





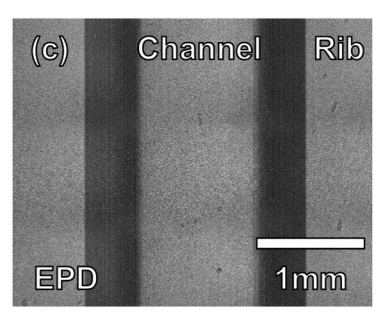


Fig. 5. Stitched confocal laser microscopy images of rib-channel structures coated by (a) APS, (b) WPS, and (c) EPD. Samples in the state prior to SOC stack integration.

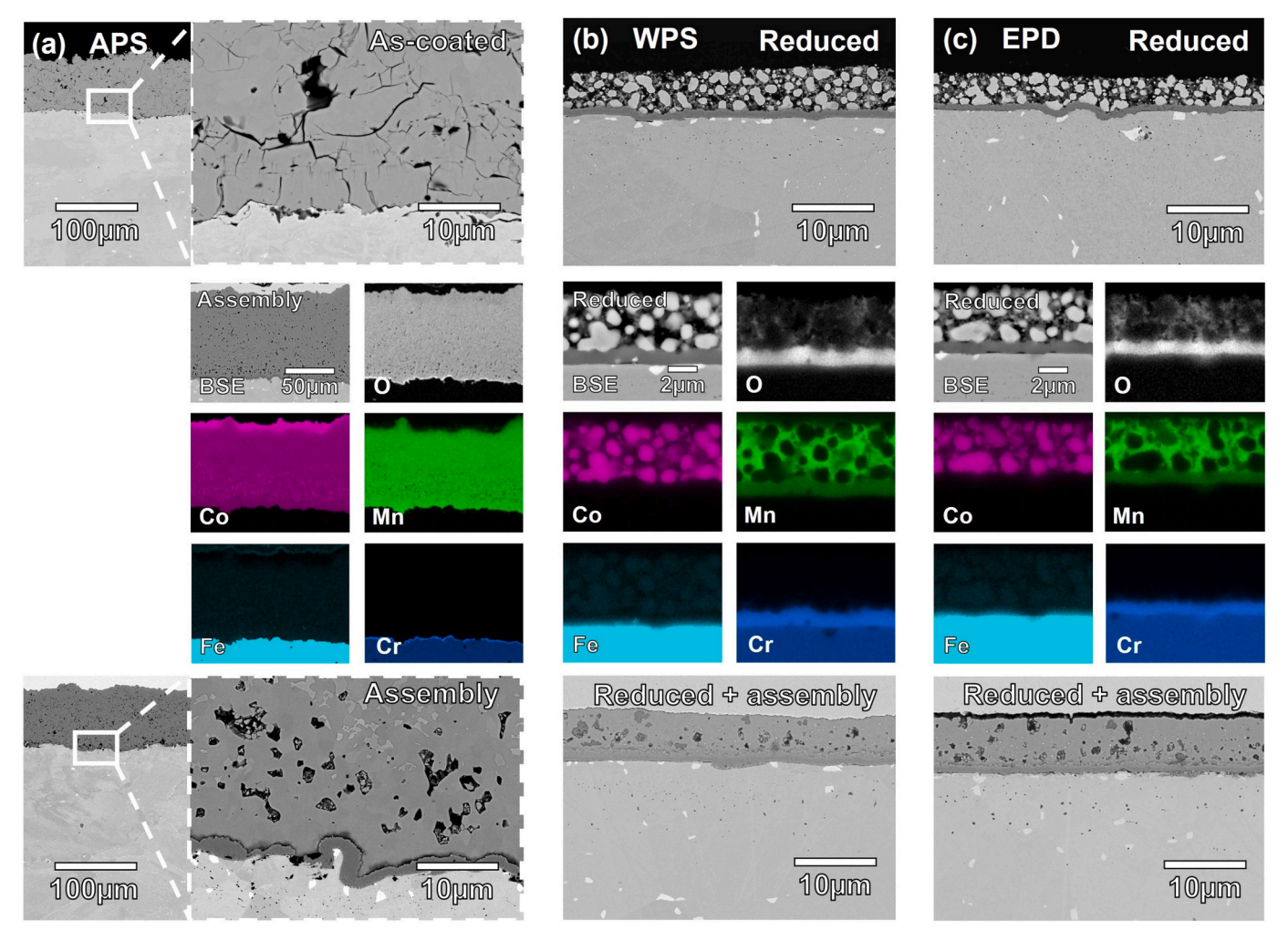


Fig. 6. SEM images of cross sections highlighting the relevant processing states of the three MCF coating types – (a) APS, (b) WPS and (c) EPD – on flat Crofer22H substrates; Fe signals enhanced by +50 % to visualize the localization of Fe within the coating.

Notably, there is an indication that the WPS and EPD coatings offer a more pronounced corrosion protection compared to the established APS coating. For the APS-coated samples, a pure  $Cr_2O_3$  scale forms beneath the coating. Its thickness varies locally but remains slightly thinner than the chromia layer observed on the uncoated Crofer22H substrate. By contrast, for the WPS- and EPD-coated specimens, the oxide scale evolves into a bi-layered structure, similar to the bare steel but significantly thinner. Here, a native  $Cr_2O_3$  layer is covered by an additional  $(Mn,Cr(Co))_3O_4$  spinel layer, providing an extended link between substrate and coating. Although direct chromium evaporation measurements were not part of the present study, the observed Cr localization and protective oxide morphologies strongly indicate the suppression of volatile species formation by all three coating types.

The reduced oxidation rates observed in WPS and EPD coatings are likely due to Zr incorporation from the coating into the oxide scale. This behavior is associated with the reactive element effect and could be attributed to unintentional Zr contamination during powder synthesis or powder and suspension processing [65]. The underlying mechanism involves the segregation of elements, such as Zr, occurring at the grain boundaries within the oxide layer and thereby impeding the Cr outward diffusion.

Indeed, distinct differences in microstructural evolution and protective behavior are observed among the three coating types. Nevertheless, it is clearly demonstrated that, through proper tailoring of heat treatments – aligned with the thermal processing conditions of a SOC stack –, well-adhering and protective coatings can be achieved, even

over longer exposure durations. Considering the established long-term performance of MCF-APS coatings reported in literature, it can be concluded that all three coating types – APS, WPS, and EPD – are suitable candidates for inclusion in in-depth environmental sustainability assessments for SOC interconnect applications.

#### 3.3. Environmental life cycle assessment results

Fig. 8 shows the environmental characterization results for each coating system, facilitating the identification of the environmental hotspots and possible areas of improvement in relation to each coating technique. In this regard, the MCF powder, argon, and electricity were identified as the three environmental hotspots for the three assessed coating methods. Processes with low contribution (under 5 %) to the assessed environmental indicators were grouped under the category "Rest" in Fig. 8. It should be noted that the magnitude of the environmental characterization results in Fig. 8a suggests the importance of including coating-related impacts besides those of the substrate, e.g. steel, when coated materials are involved in LCA studies. It also suggests the importance of further progress in coating science and technology with special regards to the environmental implications [63].

As shown in Fig. 8a, APS would involve the worst environmental performance among the three coating techniques in the four indicators under study. According to Fig. 8b, which presents the share percentage of each process to the potential environmental impacts, the unfavorable performance of APS would be closely linked to its demand for MCF

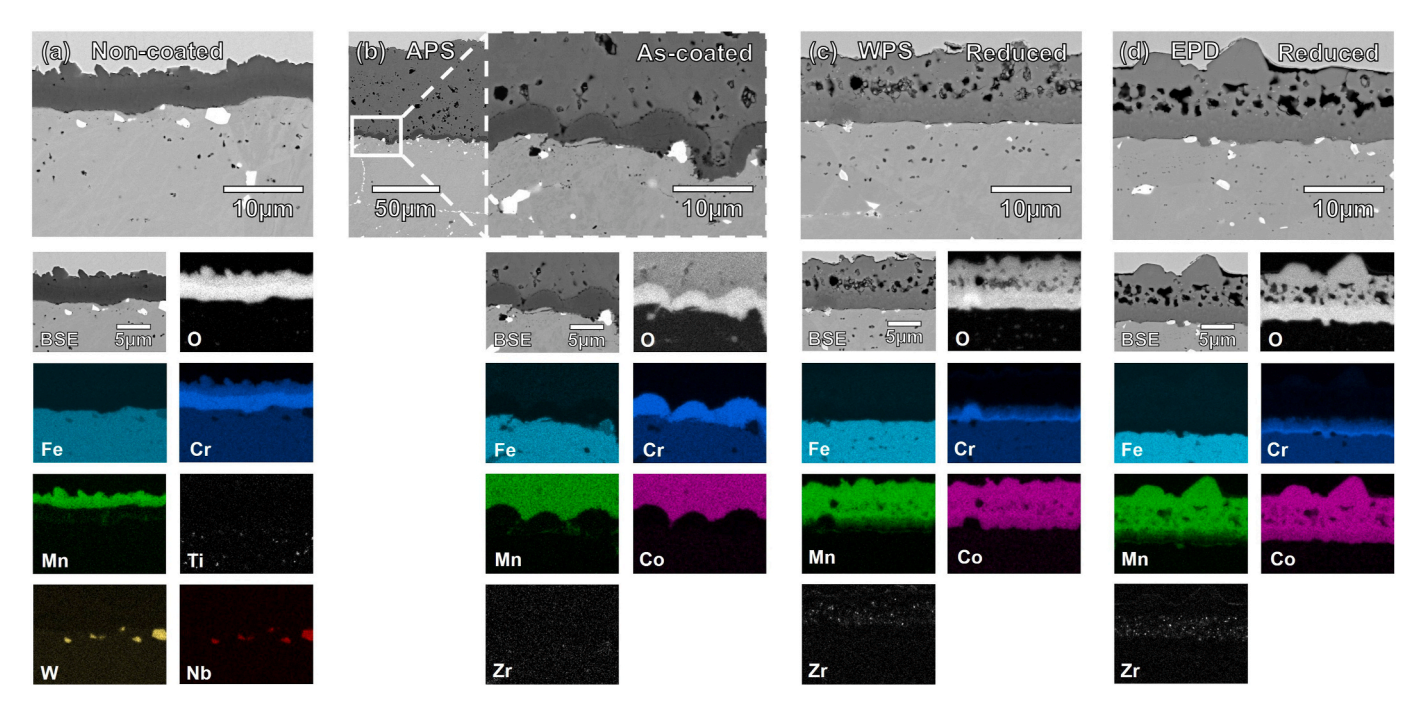


Fig. 7. SEM images and EDS mappings of Crofer22H substrates after 3000 h exposure at 800 °C in air. (a) Bare, (b) APS-, (c) WPS- and (d) EPD-coated steel as cross sections highlighting the oxide scale formation below the MCF coatings. W and Nb indicate Laves phases, and Ti corresponds to TiO precipitates, both characteristics of Crofer22H.

powder as it dominates every indicator with contribution percentages higher than 50 %. Notably, MCF's impact would reach a maximum contribution of 97 % for the use of minerals and metals. These effects could be mitigated with continuous research for the APS coating technique in terms of material efficiency and by advancements to reduce critical raw materials in protective coatings for metals.

For WPS and EPD, the environmental profiles were found to be similar, with a slightly better performance for EPD in all four indicators. In these two techniques, argon and electricity were generally found to play a more dominant role than MCF. This is linked to the fact that the amounts of MCF powder used in WPS and EPD are much lower than in the APS case (Table 2). The higher MCF consumption in APS is associated with the higher thickness of the coating layer (one order of magnitude more than in the other two techniques) and the lower coating efficiency due to direct over-spraying and powder falling while sprayed over the substrate.

Continuous development and innovations are necessary to achieve better performance and reduce the reported environmental impacts. For APS, as the most established and used method out of the three under study, reducing the amount of powder consumption and/or changing its composition should be pursued. Efforts to recycle the undeposited powder – pending feasibility studies – could significantly improve process efficiency and substantially influence the assessment outcomes.

For WPS and EPD, optimization of synthesis processes and steps could lower energy consumption leading to a more favorable environmental profile and wider industrial use. Additionally, adjustments on operational parameters (as the reducing temperature and dwell time) or alternative energy sources could also contribute to impact reduction. Moreover, further research and experimental work on replacing argon with nitrogen could be pursued, as this substitution could significantly improve environmental performance across all indicators [63].

All in all, the LCA results indicate that EPD, followed by WPS, is the most environmentally friendly coating method among the three assessed ones, whereas further efforts should be directed towards increasing material efficiency in APS. Optimizing the energy-intensive process of reduction for WPS and EPD could notably lower the system energy consumption and its associated impacts. Looking ahead, the increased

integration of renewable energy sources into electricity production mixes and advancements in coating technology are expected to enhance the environmental performance of these processes. In this sense, LCA studies should be regularly updated to reflect emerging innovations and improvements concerning the three identified environmental hotspots.

#### 4. Conclusion

From a technical standpoint, it can be concluded that all three coating types investigated (APS, WPS, EPD) are suitable for application as protective layers on SOC interconnects. Minor differences in long-term performance may arise due to variations in microstructure and layer thickness – particularly on real interconnect components – resulting from the respective deposition method. Nevertheless, findings from previous studies, including implementation at the SOC stack level, along with the results demonstrated in this work, confirm that all three coating approaches – using a state-of-the-art (Mn,Co,Fe)<sub>3</sub>O<sub>4</sub> spinel material applied to high-performance Crofer-type steels – represent highly promising options.

For the material systems considered in this study, all three coating types exhibited structural stability and proved effective protection against outward migration of chromium species. While all three coatings demonstrate effectiveness in limiting uncontrolled steel oxidation, the deposition techniques that are comparatively newer to SOC interconnect coating research – WPS and EPD – tend to result in the formation of thinner oxide scales compared to the established APS method. This might be beneficial in terms of electrical performance and could likely be attributed to the reactive element effect associated with the incorporation of Zr, present in the coating material, into the oxide scale. However, this assumption concerning the mechanism and its performance impact requires further detailed investigation from a technical perspective, particularly through in-depth analysis and long-term studies

Finally, from an environmental perspective, EPD and – to a similar extent – WPS clearly outperform APS in all environmental impact indicators, especially in terms of use of minerals and metals due to the comparatively high amount of MCF powder used in the APS technique.

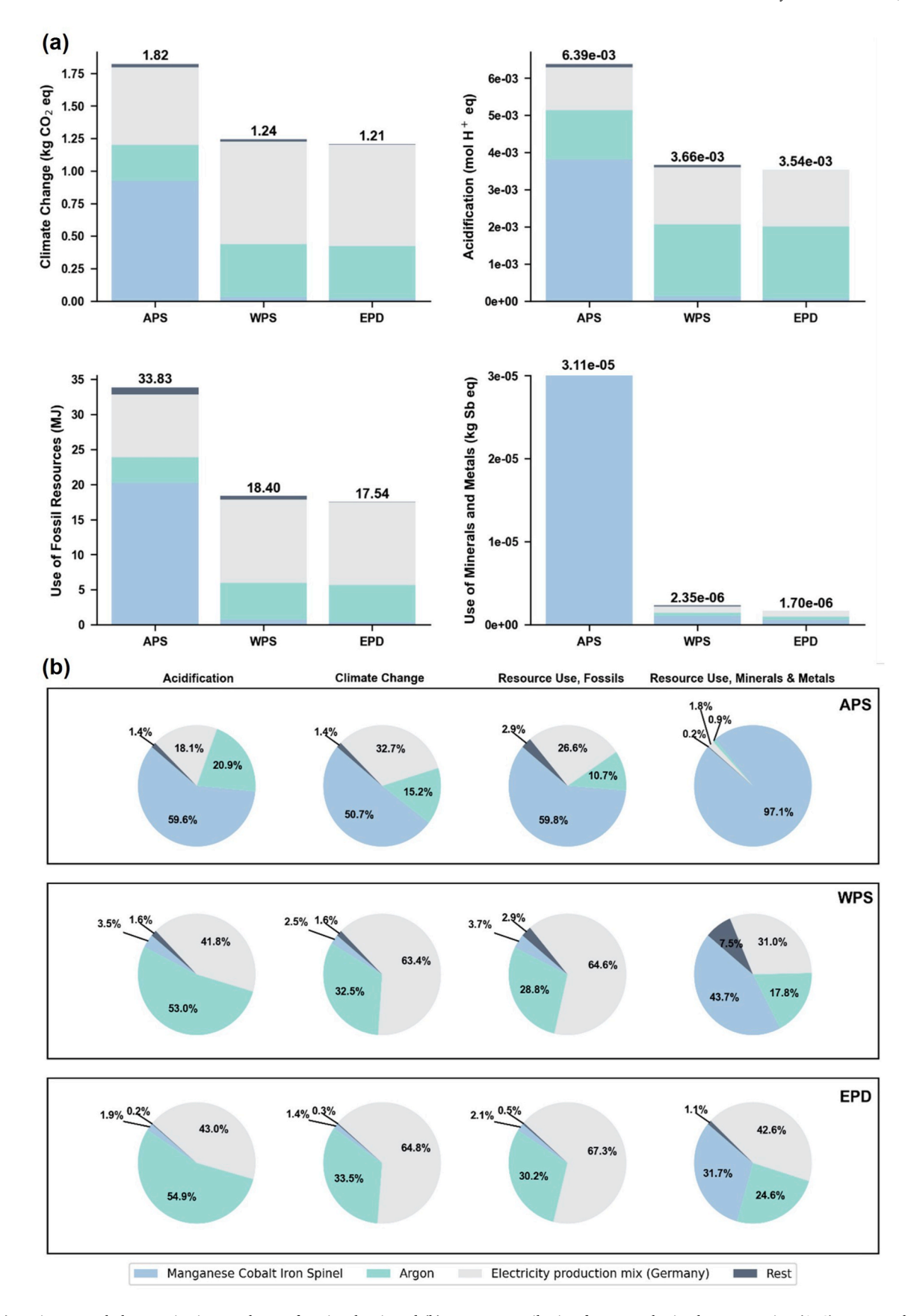


Fig. 8. (a) Environmental characterization results per functional unit and (b) process contribution for atmospheric plasma spraying (APS), wet powder spraying (WPS), and electrophoretic deposition (EPD).

Nevertheless, further improvement by acting on the identified environmental hotspots (e.g. optimization of energy-intensive steps such as the reduction process, increased use of renewable electricity, and argon replacement) is required given the relevance of coating-related impacts found in this study. Progress in coating science and technology should contribute in this direction. Overall, this study showcases that components with similar technical performance can show large differences in their sustainability impact.

#### CRediT authorship contribution statement

Martin Hilger: Writing – original draft, Validation, Methodology, Investigation, Formal analysis, Data curation, Conceptualization. Khaled El Jardali: Writing – original draft, Validation, Methodology, Investigation, Formal analysis, Data curation, Conceptualization. Vafa Feyzi: Writing – review & editing, Validation, Methodology, Investigation, Formal analysis, Data curation, Conceptualization. Daniil Vakhrameev: Writing – review & editing, Investigation, Data curation. Dmitry Naumenko: Writing – review & editing, Supervision, Resources. Ruth Schwaiger: Writing – review & editing, Supervision. Diego Iribarren: Writing – review & editing, Supervision, Methodology, Funding acquisition, Conceptualization. Christian Lenser: Writing – review & editing, Supervision, Resources, Project administration, Funding acquisition, Conceptualization. Olivier Guillon: Writing – review & editing, Supervision. Norbert H. Menzler: Writing – review & editing, Supervision, Resources, Funding acquisition.

#### **Brief summary**

This study compares three industrially relevant coating processes – atmospheric plasma spraying, wet powder spraying, and electrophoretic deposition – for their suitability in applying protective Mn-Co spinel coatings on solid oxide cell interconnects. Comprehensive characterization demonstrates all methods achieve uniform, adherent, and protective layers after stack-relevant thermal treatments. From a sustainability perspective, the newer suspension-based methods – particularly electrophoretic deposition – show substantial environmental advantages, as highlighted by the accompanying life cycle assessment.

# Declaration of generative AI and AI-assisted technologies in the writing process

During the preparation of this work the authors used ChatGPT by OpenAI in order to improve the clarity and language of the manuscript. After using this service, the authors reviewed and edited the content as needed and take full responsibility for the content of the publication.

#### Declaration of competing interest

The authors declare that they have no known competing financial interests or personal relationships that could have appeared to influence the work reported in this paper.

#### Acknowledgements

We gratefully acknowledge the colleagues who contributed to this work through practical assistance, data acquisition, resources, and discussions, including: Dr. E. Wessel (IMD-1), Dr. D. Grüner (IMD-1), H. Cosler (IMD-1), A. Kick (IMD-1), Dr. D. Sebold (IMD-2), M. Xhonneux (IMD-2), J.-P. Treitz (IMD-2), Dr. A. Schwiers (IMD-2), Prof. Dr. R. Vaβen (IMD-2), K.-H. Rauwald (IMD-2), F. Kurze (IMD-2), A. Hilgers (IMD-2), V. Bader (IMD-2).

The authors gratefully acknowledge funding from the European Union's Horizon Europe research and innovation programme under grant agreement  $N^{\circ}101058784$ .

#### Data availability

Data will be made available on request.

#### References

- [1] A. Hauch, R. Küngas, P. Blennow, A.B. Hansen, J.B. Hansen, B.V. Mathiesen, et al., Recent advances in solid oxide cell technology for electrolysis, Science 370 (6513) (2020 Oct 9) eaba6118.
- [2] E.D. Wachsman, D. Oh, E. Armstrong, D.W. Jung, C. Kan, Mechanistic understanding of Cr poisoning on La0.6Sr0.4Co0.2Fe0.8O3-δ (LSCF), ECS Trans. 25 (2) (2009 Sep 25) 2871–2879.
- [3] N. Ni, S.J. Cooper, R. Williams, N. Kemen, D.W. McComb, S.J. Skinner, Degradation of (La0.68r0.4)0.95 (Co0.2 Fe0.8)O3-8 solid oxide fuel cell cathodes at the nanometer scale and below, ACS Appl. Mater. Interfaces 8 (27) (2016 Jul 13) 17360-17370
- [4] T. Horita, Chromium poisoning for prolonged lifetime of electrodes in solid oxide fuel cells - review, Ceram. Int. 47 (6) (2021 Mar) 7293–7306.
- [5] M.J. Reddy, B. Kamecki, B. Talic, E. Zanchi, F. Smeacetto, J.S. Hardy, et al., Experimental review of the performances of protective coatings for interconnects in solid oxide fuel cells, J. Power Sources 568 (2023 Jun) 232831.
- [6] J.C.W. Mah, A. Muchtar, M.R. Somalu, M.J. Ghazali, Metallic interconnects for solid oxide fuel cell: a review on protective coating and deposition techniques, Int. J. Hydrogen Energy 42 (14) (2017 Apr) 9219–9229.
- [7] J. Mao, E. Wang, H. Wang, M. Ouyang, Y. Chen, H. Hu, et al., Progress in metal corrosion mechanism and protective coating technology for interconnect and metal support of solid oxide cells, Renew. Sustain. Energy Rev. 185 (2023 Oct) 113597.
- [8] Y. Xie, W. Qu, B. Yao, N. Shaigan, L. Rose, Dense protective coatings for SOFC interconnect deposited by spray pyrolysis, ECS Trans. 26 (1) (2010 May 12) 357–362.
- [9] S.I. Lee, J. Hong, H. Kim, J.W. Son, J.H. Lee, B.K. Kim, et al., Highly dense Mn-Co spinel coating for protection of metallic interconnect of solid oxide fuel cells, J. Electrochem. Soc. 161 (14) (2014) F1389–F1394.
- [10] H. Falk-Windisch, J. Claquesin, J.E. Svensson, J. Froitzheim, The effect of metallic Co-coating thickness on ferritic stainless steels intended for use as interconnect material in intermediate temperature solid oxide fuel cells, Oxid. Metals 89 (1–2) (2018 Feb) 233–250.
- [11] J.H. Zhu, D.A. Chesson, Y.T. Yu, Review—(Mn,Co)<sub>3</sub> O<sub>4</sub> -based spinels for SOFC interconnect coating application, J. Electrochem. Soc. 168 (11) (2021 Nov 1) 114519.
- [12] Z. Zhu, C. Darl-Uzu, U. Pal, S. Gopalan, A.M. Hussain, N. Dale, et al., Comparison of Cu–Mn and Mn–Co spinel coatings for solid oxide fuel cell interconnects, Int. J. Hydrogen Energy 47 (87) (2022 Oct) 36953–36963.
- [13] S.N. Basu, Z. Zhu, J.R. Mulligan, U.B. Pal, S. Gopalan, A.M. Hussain, et al., Electrophoretically deposited protective Cu-Mn and Mn-Co spinel coatings for solid oxide fuel cell interconnects, in: ECS Transactions 111, 2023, pp. 2233–2242. Boston, USA
- [14] Y. Jin, W. Hao, M. Guo, M. Yu, Y. Guo, X. Liu, et al., Investigation of CuxMn3-xO4 coatings for solid oxide fuel cell interconnect applications, Ceram. Int. 49 (17) (2023 Sep) 27716–27723.
- [15] L. Blum, P. Batfalsky, Q. Fang, L.G.J. De Haart, J. Malzbender, N. Margaritis, et al., SOFC stack and system development at Forschungszentrum Jülich, J. Electrochem. Soc. 162 (10) (2015) F1199–F1205.
- [16] S. Harboe, A. Schreiber, N. Margaritis, L. Blum, O. Guillon, N.H. Menzler, Manufacturing cost model for planar 5 kWel SOFC stacks at Forschungszentrum Jülich, Int. J. Hydrogen Energy 45 (15) (2020 Mar) 8015–8030.
- [17] P. Gannon, M. Deibert, P. White, R. Smith, H. Chen, W. Priyantha, et al., Advanced PVD protective coatings for SOFC interconnects, Int. J. Hydrogen Energy 33 (14) (2008 Jul) 3991–4000.
- [18] J. Froitzheim, S. Canovic, M. Nikumaa, R. Sachitanand, L.G. Johansson, J. E. Svensson, Long term study of Cr evaporation and high temperature corrosion behaviour of Co coated ferritic steel for solid oxide fuel cell interconnects, J. Power Sources 220 (2012 Dec) 217–227.
- [19] M.J.G. Vargas, M. Zahid, F. Tietz, A. Aslanides, Use of SOFC metallic interconnect coated with spinel protective layers using the APS technology, ECS Trans. 7 (1) (2007 May 25) 2399–2405.
- [20] R. Vaßen, H. Kaßner, A. Stuke, F. Hauler, D. Hathiramani, D. Stöver, Advanced thermal spray technologies for applications in energy systems, Surf. Coating. Technol. 202 (18) (2008 Jun) 4432–4437.
- [21] J. Cao, Y. Zheng, W. Zhang, B. Yu, Plasma spray coating on interconnector toward promoted solid oxide fuel cells and solid oxide electrolysis cells, Front. Energy 18 (3) (2024 Jun) 390–398.
- [22] N.H. Menzler, D. Sebold, O. Guillon, Post-test characterization of a solid oxide fuel cell stack operated for more than 30,000 hours: the cell, J. Power Sources 374 (2018 Jan) 69–76.
- [23] Matlab Inc. [Internet], How consumer goods coatings protect your products. htt ps://matlabinc.com/consumer-goods-powder-coating/, 2025.
- [24] SpecialChem [Internet], Applications & uses of powder, Coatings (2025) [cited 2025 Apr 13]. Available from: https://coatings.specialchem.com/selection-gui de/powder-coatings-formulation-tips/key-applications.
- [25] A.R. Boccaccini, S. Keim, R. Ma, Y. Li, I. Zhitomirsky, Electrophoretic deposition of biomaterials, J R Soc Interface 7 (suppl\_5) (2010 Oct 6) [Internet] [cited 2025 Apr 13];Available from: https://royalsocietypublishing.org/doi/10.1098/rsif.2010 .0156.focus.

- [26] A.R. Boccaccini, J.H. Dickerson, Electrophoretic deposition: fundamentals and applications, J. Phys. Chem. B 117 (6) (2013 Feb 14), 1501–1501.
- [27] M. Wolff, A. Schwiers, K. Wilkner, D. Sebold, N.H. Menzler, Wet powder spraying a versatile and highly effective technique for the application of spinel-type protective coatings on SOC interconnects, J. Power Sources 592 (2024 Feb) 233931.
- [28] A.G. Sabato, E. Zanchi, S. Molin, G. Cempura, H. Javed, K. Herbrig, et al., Mn-Co spinel coatings on Crofer 22 APU by electrophoretic deposition: up scaling, performance in SOFC stack at 850 °C and compositional modifications, J. Eur. Ceram. Soc. 41 (8) (2021 Jul) 4496–4504.
- [29] E. Zanchi, A.G. Sabato, M.C. Monterde, L. Bernadet, M. Torrell, J.A. Calero, et al., Electrophoretic deposition of MnCo2O4 coating on solid oxide cell interconnects manufactured through powder metallurgy, Mater. Des. 227 (2023 Mar) 111768.
- [30] R. Sachitanand, M. Sattari, J.E. Svensson, J. Froitzheim, Evaluation of the oxidation and Cr evaporation properties of selected FeCr alloys used as SOFC interconnects, Int. J. Hydrogen Energy 38 (35) (2013 Nov) 15328–15334.
- [31] Z.W. Hsiao, B. Kuhn, D. Chen, L. Singheiser, J.C. Kuo, D.Y. Lin, Characterization of Laves phase in Crofer 22 H stainless steel, Micron 74 (2015 Jul) 59–64.
- [32] B. Kuhn, C.A. Jimenez, L. Niewolak, T. Hüttel, T. Beck, H. Hattendorf, et al., Effect of Laves phase strengthening on the mechanical properties of high Cr ferritic steels for solid oxide fuel cell interconnect application, Mater. Sci. Eng., A 528 (18) (2011 Jul) 5888–5899.
- [33] VDM Metals, Crofer22APU Safety data sheet. https://www.vdm-metals.com/fileadmin/user\_upload/Downloads/Data\_Sheets/Data\_Sheet\_VDM\_Crofer\_22\_APU.pd f. 2022.
- [34] VDM Metals, Crofer22H Safety data sheet. https://www.vdm-metals.com/filea dmin/user\_upload/Downloads/Data\_Sheets/Data\_Sheet\_VDM\_Crofer\_22\_H.pdf, 2021
- [35] X. Montero, F. Tietz, D. Sebold, H.P. Buchkremer, A. Ringuede, M. Cassir, et al., MnCo1.9Fe0.1O4 spinel protection layer on commercial ferritic steels for interconnect applications in solid oxide fuel cells, J. Power Sources 184 (1) (2008 Sep) 172–179.
- [36] V. Miguel-Pérez, A. Martínez-Amesti, M.L. Nó, A. Larrañaga, M.I. Arriortua, The effect of doping (Mn,B) 3 O 4 materials as protective layers in different metallic interconnects for Solid Oxide Fuel Cells, J. Power Sources 243 (2013 Dec) 419–430.
- [37] N. Grünwald, D. Sebold, Y.J. Sohn, N.H. Menzler, R. Vaßen, Self-healing atmospheric plasma sprayed Mn1.0Co1.9Fe0.1O4 protective interconnector coatings for solid oxide fuel cells, J. Power Sources 363 (2017 Sep) 185–192.
- [38] L. Besra, M. Liu, A review on fundamentals and applications of electrophoretic deposition (EPD), Prog. Mater. Sci. 52 (1) (2007 Jan) 1–61.
- [39] I. Corni, M.P. Ryan, A.R. Boccaccini, Electrophoretic deposition: from traditional ceramics to nanotechnology, J. Eur. Ceram. Soc. 28 (7) (2008 Jan) 1353–1367.
- [40] P.L. Fauchais, J.V.R. Heberlein, M.I. Boulos, Thermal Spray Fundamentals: from Powder to Part, Springer US, Boston, MA, 2014 [Internet][cited 2025 Apr 22]. Available from: https://link.springer.com/10.1007/978-0-387-68991-3.
- [41] B.K. Swain, S.S. Mohapatra, A. Pattanaik, S.K. Samal, S.K. Bhuyan, K. Barik, et al., Sensitivity of process parameters in atmospheric plasma spray coating, JTSE 1 (1) (2018) 1–6.
- [42] R. Steinberger-Wilckens, L. Blum, H.P. Buchkremer, L.G.J. De Haart, M. Pap, R. W. Steinbrech, et al., Recent results in solid oxide fuel cell development at Forschungszentrum juelich, ECS Trans. 25 (2) (2009 Sep 25) 213–220.
- [43] L. Blum, U. Packbier, I.C. Vinke, L.G.J. De Haart, Long-term testing of SOFC stacks at Forschungszentrum Jülich, Fuel Cells 13 (4) (2013 Aug) 646–653.
- [44] L. Blum, L.G.J. de Haart, J. Malzbender, N. Margaritis, N.H. Menzler, Anode-supported solid oxide fuel cell achieves 70 000 hours of continuous operation, Energy Technol. 4 (8) (2016 Aug) 939–942.
- [45] R. Vaßen, N. Grünwald, D. Marcano, N.H. Menzler, R. Mücke, D. Sebold, et al., Aging of atmospherically plasma sprayed chromium evaporation barriers, Surf. Coating. Technol. 291 (2016 Apr) 115–122.
- [46] A. Ruder, H.P. Buchkremer, H. Jansen, W. Malléner, D. Stöver, Wet powder spraying—a process for the production of coatings, Surf. Coating. Technol. 53 (1) (1992 Jul) 71–74.

- [47] L. Zhao, M. Bram, H. Buchkremer, D. Stover, Z. Li, Preparation of TiO composite microfiltration membranes by the wet powder spraying method, J. Membr. Sci. 244 (1–2) (2004 Nov 15) 107–115.
- [48] N.H. Menzler, D. Sebold, Y.J. Sohn, S. Zischke, Post-test characterization of a solid oxide fuel cell after more than 10 years of stack testing, J. Power Sources 478 (2020 Dec) 228770.
- [49] B. Talic, H. Falk-Windisch, V. Venkatachalam, P.V. Hendriksen, K. Wiik, H.L. Lein, Effect of coating density on oxidation resistance and Cr vaporization from solid oxide fuel cell interconnects, J. Power Sources 354 (2017 Jun) 57–67.
- [50] E. Zanchi, A.G. Sabato, S. Molin, G. Cempura, A.R. Boccaccini, F. Smeacetto, Recent advances on spinel-based protective coatings for solid oxide cell metallic interconnects produced by electrophoretic deposition, Mater. Lett. 286 (2021 Mar) 129229
- [51] Ł. Mazur, A. Gil, B. Kamecki, K. Domaradzki, M. Bik, P. Zając, et al., On the possibility of improving the oxidation resistance of high-chromium ferritic stainless steel using reactive element oxide nanoparticles, Metall. Mater. Trans. A 55 (7) (2024 Jul) 2555–2570.
- [52] B. Wang, K. Li, J. Liu, T. Zhang, T. Yang, N. Zhang, Promoting electric conductivity of MnCo spinel coating by doping transition metals (Cu, Fe) or rare-earth elements (La, Y) for solid oxide fuel cell interconnect, Int. J. Hydrogen Energy 61 (2024 Apr) 216–225.
- [53] S.H. Kim, D. Kim, S.U. Oh, J.A. Lee, Y.W. Heo, J.H. Lee, Enhanced performance of Zn-modified (MnCo)1.5O4 spinel coatings: investigating critical properties for SOFC interconnect materials, Int. J. Hydrogen Energy 102 (2025 Feb) 444–451.
- [54] L. Dusoulier, R. Cloots, B. Vertruyen, R. Moreno, O. Burgos-Montes, B. Ferrari, YBa2Cu3O7—x dispersion in iodine acetone for electrophoretic deposition: surface charging mechanism in a halogenated organic media, J. Eur. Ceram. Soc. 31 (6) (2011 Jun) 1075–1086.
- [55] F. Smeacetto, A. De Miranda, S. Cabanas Polo, S. Molin, D. Boccaccini, M. Salvo, et al., Electrophoretic deposition of Mn1.5Co1.5O4 on metallic interconnect and interaction with glass-ceramic sealant for solid oxide fuel cells application, J. Power Sources 280 (2015 Apr) 379–386.
- [56] S. Molin, A.G. Sabato, M. Bindi, P. Leone, G. Cempura, M. Salvo, et al., Microstructural and electrical characterization of Mn-Co spinel protective coatings for solid oxide cell interconnects, J. Eur. Ceram. Soc. 37 (15) (2017 Dec) 4781–4791.
- [57] S. Molin, A.G. Sabato, H. Javed, G. Cempura, A.R. Boccaccini, F. Smeacetto, Co-deposition of CuO and Mn1.5Co1.5O4 powders on Crofer22APU by electrophoretic method: structural, compositional modifications and corrosion properties, Mater. Lett. 218 (2018 May) 329–333.
- [58] A.G. Sabato, S. Molin, H. Javed, E. Zanchi, A.R. Boccaccini, F. Smeacetto, In-situ Cu-doped MnCo-spinel coatings for solid oxide cell interconnects processed by electrophoretic deposition, Ceram. Int. 45 (15) (2019 Oct) 19148–19157.
- [59] E. Zanchi, S. Molin, A.G. Sabato, B. Talic, G. Cempura, A.R. Boccaccini, et al., Iron doped manganese cobaltite spinel coatings produced by electrophoretic codeposition on interconnects for solid oxide cells: microstructural and electrical characterization, J. Power Sources 455 (2020 Apr) 227910.
- [60] International Organization for Standardization, ISO 14040:2006 Environmental Management – Life Cycle Assessment – Principles and Framework, 2006. Geneva.
- [61] K. El Jardali, V. Feyzi, D. Iribarren, J. Dufour, Sustainability Characterisation of the Electrode and Interconnect Concepts Based on Advanced Coating Technologies, NOUVEAU project, 2024.
- [62] R. Scataglini, M. Wei, A. Mayyas, S.H. Chan, T. Lipman, M. Santarelli, A direct manufacturing cost model for solid-oxide fuel cell stacks, Fuel Cells 17 (6) (2017 Dec) 825–842.
- [63] G. Wernet, C. Bauer, B. Steubing, J. Reinhard, E. Moreno-Ruiz, B. Weidema, The ecoinvent database version 3 (part I): overview and methodology, Int. J. Life Cycle Assess. 21 (9) (2016 Sep) 1218–1230.
- [64] European Commission, Joint Research Centre, Updated characterisation and normalisation factors for the environmental footprint 3.1 method. [Internet], Publications Office, 2023, https://data.europa.eu/doi/10.2760/798894.
- [65] B.A. Pint, Experimental observations in support of the dynamic-segregation theory to explain the reactive-element effect, Oxid. Metals 45 (1–2) (1996 Feb) 1–37.